

Fig.12 Expected Data of Capacitance change at $\theta = 60^\circ\text{C}$

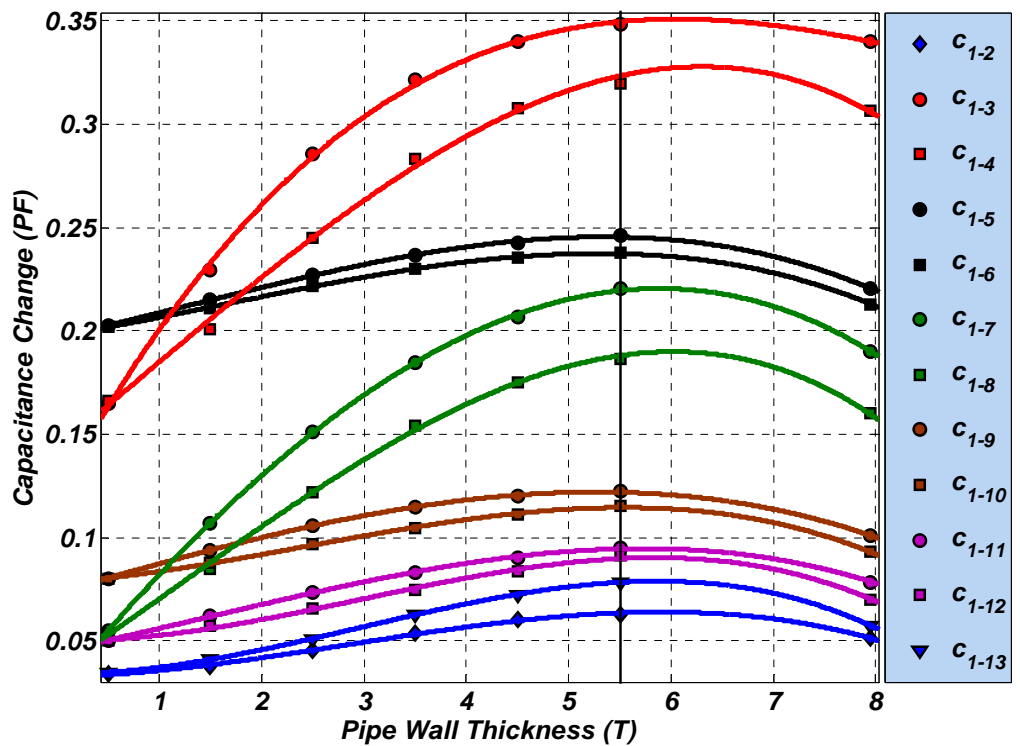


Fig.13 Expected Data of Capacitance change at $\theta = 80^\circ\text{C}$

Table 3. Corrosion rate Constants (a_{ij}), (b_{ij}), (k_{ij}) and (h_{ij}) at $\theta = 25^{\circ}\text{C}, 40^{\circ}\text{C}, 60^{\circ}\text{C}$ and 80°C

	θ	C₁₋₂	C₁₋₃	C₁₋₄	C₁₋₅	C₁₋₆	C₁₋₇	C₁₋₈	C₁₋₉	C₁₋₁₀	C₁₋₁₁	C₁₋₁₂	C₁₋₁₃
a_{ij}	* 25°C	-7867	-1107	-1533	-2860	-3277	-4094	-4718	-5964	-6254	-6823	-7072	-7643
	** 40°C	-7713	-952	-1376	-2691	-3125	-3942	-4562	-5805	-6100	-6668	-6918	-7485
	** 60°C	-7396	-632	-1054	-2372	-2806	-3623	-4241	-5493	-5785	-6353	-6593	-7173
	** 80°C	-7172	-413	-832	-2158	-2581	-3411	-4028	-5272	-5552	-6126	-6372	-6951
$b_{ij} \times 10^{-4}$	* 25°C	-0.1907	-0.1987	-0.1967	-0.1938	-0.1921	-0.1953	-0.1928	-0.1973	-0.1980	-0.1972	-0.1924	-0.1983
	** 40°C	-0.1923	-0.1997	-0.1955	-0.1923	-0.1912	-0.1942	-0.1936	-0.1922	-0.1911	-0.1958	-0.1966	-0.1998
	** 60°C	-0.1979	-0.1982	-0.1927	-0.1931	-0.1953	-0.1966	-0.1919	-0.1925	-0.1995	-0.1969	-0.1939	-0.1974
	** 80°C	-0.1958	-0.1959	-0.1986	-0.1924	-0.1972	-0.1939	-0.1923	-0.1982	-0.1988	-0.1917	-0.1987	-0.1961
	Avg.	-0.1942	-0.1981	-0.1959	-0.1929	-0.194	-0.195	-0.1926	-0.1951	-0.1969	-0.1954	-0.1954	-0.1979
	S.D.	0.0033	0.0016	0.0025	0.0007	0.0028	0.0012	0.0007	0.0031	0.0039	0.0025	0.0028	0.0016
k_{ij}	* 25°C	7867	1107	1533	2860	3277	4094	4718	5964	6254	6823	7072	7643
	** 40°C	7713	952	1376	2691	3125	3942	4562	5805	6100	6668	6918	7485
	** 60°C	7396	632	1054	2372	2806	3623	4241	5493	5785	6353	6593	7173
	** 80°C	7172	413	832	2158	2581	3411	4028	5272	5552	6126	6372	6951
$h_{ij} \times 10^{-4}$	* 25°C	0.1921	0.1986	0.1977	0.1927	0.1960	0.1964	0.1976	0.1978	0.1903	0.1929	0.1995	0.1973
	** 40°C	0.1956	0.1945	0.1945	0.1941	0.1921	0.1949	0.1932	0.1998	0.1982	0.1941	0.1925	0.1946
	** 60°C	0.1962	0.1969	0.1987	0.1911	0.1982	0.1962	0.1925	0.1999	0.1913	0.1964	0.1987	0.1997
	** 80°C	0.1933	0.1948	0.1964	0.1987	0.1949	0.1942	0.1928	0.1983	0.1920	0.1981	0.1922	0.1921
	Avg.	0.1943	0.1962	0.1968	0.1942	0.1953	0.1954	0.194	0.199	0.193	0.1954	0.1957	0.1959
	S.D.	0.0019	0.0019	0.0018	0.0033	0.0025	0.0011	0.0024	0.0011	0.0036	0.0023	0.0039	0.0033
C_F	* 25°C	0.9945	0.9921	0.9908	0.9369	0.9928	0.9701	0.9828	0.9628	0.9043	0.9946	0.9715	0.9932
	** 40°C	0.9994	0.9995	0.9976	0.9921	0.9948	0.9999	0.9989	0.9983	0.9855	0.9993	0.9911	0.9897
	** 60°C	0.998	0.9994	0.9946	0.9939	0.9991	0.9999	0.9921	0.9987	0.9963	0.9994	0.9993	0.9903
	** 80°C	0.9977	0.9992	0.9973	0.999	0.9993	0.9999	0.9988	0.9991	0.9984	0.9993	0.9955	0.9999

* FEM Data

** FFNN Expected Data

6. CONCLUSION

For this work, the finite element method (FEM) and artificial neural network (ANN) techniques were used for modeling and simulating the electrical capacitance tomography (ECT) sensor to detect the corrosion rates inside steel pipelines and study and predict the effect of pipeline environment temperature (θ) on the corrosion rates, the following conclusions can be drawn:

- 1) The pipeline internal corrosion is means decrease of the pipeline thickness was discussed completely by FEM numerical simulation software ANSYS. The influence of pipeline to electrode pairs decreases followed by (C₁₋₃, C₁₋₄, C₁₋₅, C₁₋₆, C₁₋₇, C₁₋₈, C₁₋₉, C₁₋₁₀, C₁₋₁₁, C₁₋₁₂, C₁₋₁₃ and C₁₋₂). Maximum capacitance change is gotten at X=6.95 mm, $\rho = 0.79$, which is beneficial for capacitance measurement. With the decrease of pipe wall thickness (X) or decrease of the radius-electrode ratio (ρ), the distortion of ECT sensor sensitivity becomes more serious.
- 2) An artificial neural network can be used as a method for simulating the ECT sensor to expect the non-FE Data of capacitance change at the pipeline environment temperature $\theta = 25^{\circ}\text{C}$, 40°C , 60°C and 80°C .
- 3) Training a neural network is heavily time consuming.
- 4) Using the exponential formula $C_{ij} = a_{ij}e^{b_{ij}X} + k_{ij}e^{h_{ij}X}$ has proved its suitability for present study, and it is found that, the deviation of the constants (b_{ij} & h_{ij}) for different pipeline environment temperature (θ) and capacitance change (C_{ij}) is negligible and it may be considered to be constant.
- 5) The value of the constants (a_{ij} & k_{ij}) were found to be depend on the pipeline environment temperature (θ) and the capacitance change (C_{ij}) with high correlation factors (C.F), as the pipeline environment temperature (θ) increases the value of (a_{ij} & k_{ij}) will decreases i.e. the pipeline environment temperature (θ) had a detrimental effect on the corrosion rates increases.

REFERENCES

- Fasching, G.E.; Smith, N.S., (1988), "High Resolution Capacitance Imaging System", US Dept. Energy, 37, DOE/METC-88/4083
- Fasching, G.E.; Smith, N.S., (1991) "A Capacitive System for 3-Dimensional Imaging of Fluidized-Beds", Rev. Sci. Instr., 62, 2243-2251
- Yang W. Q., et al., (1995a), "Development of capacitance tomographic imaging systems for oil pipeline measurements", Review of Scientific Instruments, 66(8), pp. 4326
- Yang W. Q., et al., (1995b), "Electrical capacitance tomography –from design to applications", Measurement & Control, 28(9), pp. 261-266
- Li Haiqing et al., (2000), "Special measurement technology and application", Hangzhou: Zhejiang University Press
- Yang W. Q., et al., (1999), "New AC-based capacitance tomography system", IEE proceedings: Measurement Science and Technology, 146(1), pp.47-53.
- Yang W. Q., et al., (1997), "Modelling of capacitance sensor", IEE proceedings: Measurement Science and Technology, 144(5), pp. 203-208.

Jaworski A. J., et al., (2000), "The design of an electrical capacitance tomography sensor for use with media of high dielectric permittivity", Measurement Science and Technology, 11(6), pp. 743-757

Xie, et al., (1992), "Electrical capacitance tomography for flow imaging: system model for development of image reconstruction algorithms and design of primary sensors", IEE Proceedings-G, 139(1): 89-98